

Data Reliability Analysis for Early Fault Diagnosis of Air Handling Unit (AHU)



Hasmat Malik, Shahrin Md Ayob, Nik Rumzi Nik Idris, Awang Jusoh, Fausto Pedro García Márquez, and Abdulaziz Almutairi

Abstract The objective of this chapter is to analyze the reliability of the dataset for early fault diagnosis of air handling unit (AHU) of air conditioning and mechanical ventilation/heating, ventilation, and air conditioning (ACMV/HVAC) system. In this chapter, data reliability analysis for early fault diagnosis is performed for AHU only, which includes fan degradation and return air duct leakage fault conditions. Data of the said faults are generated through the use of an expert system platform, OpenStudio (OS) and sensitivity analysis is performed to identify the most sensitive parameters with respect to the fault severity level starting from zero to 30% of deviation from healthy condition. The most sensitive parameters are selected based on the rank of sensitivity analysis. A similar procedure was performed with real data obtained from measurement. The effect of parameters due to fault conditions in AHU is analyzed in terms of consistency of increasing, decreasing, both increasing and decreasing, and no correlation. The results of the analyzed data are documented and compared.

H. Malik (✉) · S. M. Ayob · N. R. N. Idris · A. Jusoh
Department of Electrical Power Engineering, Universiti Teknologi Malaysia (UTM), Johor Bahru, Malaysia
e-mail: hasmat@utm.my

S. M. Ayob
e-mail: e-shahrin@utm.my

N. R. N. Idris
e-mail: e-nrumzi@utm.my

A. Jusoh
e-mail: awang@utm.my

F. P. G. Márquez
Ingenium Research Group, Universidad Castilla-La Mancha, 13071 Ciudad Real, Spain
e-mail: faustopedro.garcia@uclm.es

A. Almutairi
Department of Electrical Engineering, College of Engineering, Majmaah University, Al Majma'ah 11952, Saudi Arabia

Keywords Air handling unit (AHU) · Air conditioning and mechanical ventilation (ACMV) · Heating, ventilation and air conditioning (HVAC) · Data reliability · Early fault · Fault detection and diagnosis (FDD)

1 Introduction

The energy consumed for cooling contributes the most to a typical building energy consumption in tropical region like Malaysia. Faults and performance degradation in the air conditioning and mechanical ventilation/heating, ventilation, and air conditioning (ACMV/HVAC) system lead to energy wastage. As the cost of ACMV operation is already high, any efficiency losses would increase the cost further. In addition, electricity used to power the system is mainly generated from non-renewable sources in Malaysia and Singapore, which contributes to greenhouse gases when burned. As a result, there is a need for fault detection and diagnosis to minimize the impacts when a fault occurs. Faults can occur at any of the sub-systems of the ACMV and due to its size and complexity, it is a challenge to diagnose them accurately at low severity levels.

The ACMV or HVAC is a system that controls the temperature, humidity, fresh air, filtration, and movement of air through space. In Malaysia region, heating is not required, thus the system is known as ACMV, while regions that require heating use HVAC. The goal of such a system is to provide thermal comfort and acceptable indoor air quality for the occupants or to provide cooling for equipment. The ACMV can achieve this by conditioning the air through [1–5]: cooling, dehumidifying, cleaning, and ventilating. All these can be done based on the principles of thermodynamics, fluid mechanics and heat transfer. There are three subsystem that works together to perform the functions mentioned above. These three sub-systems are cooling tower, chiller plant, and AHU. Figure 1 depicts the interdependency of the three sub-systems and how heat is being transferred around the ACMV system.

The cooling tower removes the heat from the chiller plant's condenser through heat exchangers filled with water. This water loop is called the condenser water loop, the water is then pumped from the condenser to the tower. The water is cooled by pumping it up to the top of the cooling tower where the ambient air and wind can remove the heat from the water. Heat is removed from the water as it is sprayed on to thin film materials. As the water flows from the top to the bottom of the cooling tower, it is exposed to the ambient air and wind which cools it down. The cooled condenser water is then circulated back to the chiller plant's condenser to absorb heat again.

The chiller plant provides the cooling capacity for the building as the centralized cooling system. It provides cooling based on vapor compression which is the fundamental process in the refrigeration cycle. In the chiller plant, the compressor compresses the refrigerant which allows heat absorption at the evaporator and releases that heat at the condenser. The refrigerant circulates through an evaporator, compressor, condenser, and an expansion valve. A thermodynamic process at each

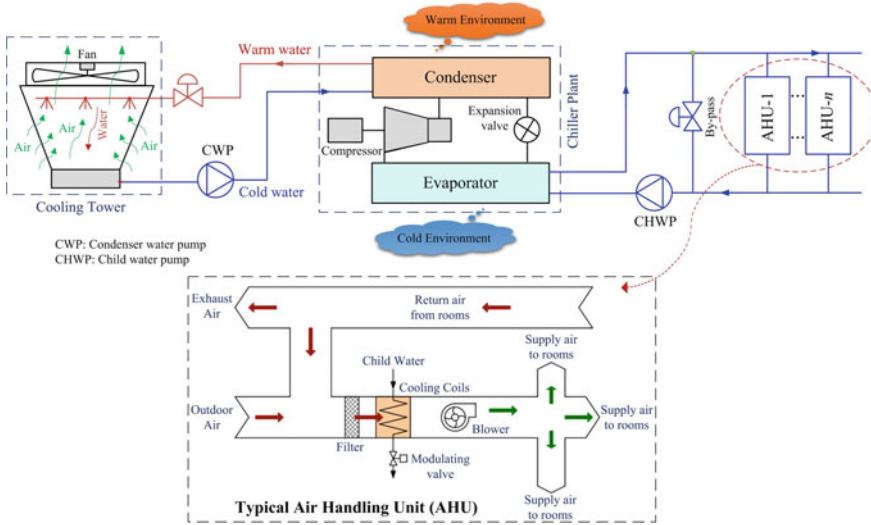


Fig. 1 Main components of central air conditioning system

component to ensure a continuous flow of cold refrigerant to absorb the heat from the chilled water loop. The cooled chilled water is then sent to the cooling coil for the AHU to cool the air.

The AHU is a system of ducts, filters, dampers, and fans to circulate cold fresh air and exhaust stale air. Fresh air is collected through an intake and cooled at the cooling coil as cold chilled water circulates the coil to absorb the heat from the air. The cooling coil dehumidifies the air as well by removing moisture in the air. The cold fresh air is then supplied to the various cooling zones in the building through the fans and ducts. Fans are used to aid in the circulation of conditioned air around the building as well as exhausting stale air through an outlet. Filters are used for cleaning and dampers regulate the amount of cold air entering each zone.

Cooling is provided through the removal of heat in spaces, the heat can be removed through radiation, convection, or conduction. The heat is transferred through a refrigeration system which uses a medium to absorb the heat and disperse it outdoors. The medium is known as the refrigerant, which can be water, air, or chemicals. This is possible by making use of a thermodynamic cycle called the refrigeration cycle. There is a compressor in the system that changes the pressure and state of the refrigerant to absorb or release heat.

Dehumidification of air drying is provided by the cooling coil as the temperature at the coil is below the dew point, thus moisture in the air will condense around the cooling coil. The moisture is then collected at the bottom of the coil and removed via piping.

Cleaning is done by air filtration at the AHU to remove particles, contaminants, vapors, and gases. This helps to remove air pollutants such as pollen and dust from the air, improving and regulating the air quality within the building. This is done by

implementing filters of various materials in the air ducts, especially the outdoor air inlets to prevent pollutants from entering the building. This also prevents ducts or fan blades from dust accumulation.

Ventilation is normally done mechanically through the AHU via the multiple fans within the duct system. Conditioned outside air is delivered into the building by a supply air fan and existing air is being exhausted to prevent carbon dioxide build-up. Ventilation is necessary as it is one of the most important factors for maintaining indoor air quality within the building. Without ventilation, stale air can happen which has an unpleasant smell and can become a health hazard for the occupants at higher levels.

ACMV has become an essential system and integrated into our society, both in residential and industrial. The ACMV system contributes to more than 60% of the total building energy consumption. Within the ACMV system, the chillers and fans are the two components that contribute significantly to energy consumption. Chiller consumes up to 55% and fans up to 35% of the total energy consumption [2–5].

Therefore, early FDD is very important for ACMV's health monitoring as well as optimal utilization of electrical energy, which is directly dependent on the optimal selection of the dataset and its severity level w.r.t. the fault condition. The main objective of this study is to analyze the severity and reliability of the dataset, which is used to detect and diagnose faults at low severity. By detecting faults at low severity, fixes, and maintenance can be done at a lower cost when compared with a more severe fault. This ensures the system operates optimally and reduces costs related to operation and maintenance. This in turn helps building owners to reduce electricity consumption and their carbon footprint.

The organization of this paper is comprised of seven sections. Section 1 represents the introduction. Brief information of AHU is represented in Sect. 2, which includes main components of the ACMV/HVAC and its related components. Section 3 represents brief information of AHU faults and its severity. The simulation of the model is shown in Sect. 4. Sections 5 and 6 represent the dataset collection and sensitivity analysis, respectively. Finally conclusion is represented in Sect. 7.

2 Brief Information of Air Handling Unit (AHU)

Figure 1 represents the main components of the central air conditioning (CAC) system, which includes mainly three sub-systems, i.e., cooling tower, chiller plant, and air handling unit (AHU).

The cooling tower is the point where the heat absorbed from the cooling zones are being dissipated into the atmosphere through the evaporative process. Warm condenser water is circulated to the top of the cooling tower, where the water is exposed and evaporated into the air passing through the cooling tower. As the water evaporates, the air absorbs heat and cools the remaining condenser water. The remaining condenser water will flow into a collection basin, where it can be pumped

back to the condenser to absorb heat at the chiller plant. There are five main components to a cooling tower, exhaust fan, drift eliminators, water distribution, fill, and basin. The hot condenser water is sprayed from the water distribution using a nozzle, it then flows on to the fill section which aids in the evaporation rate. The cooled water is then collected at the cooling tower basin which is then circulated back to the condenser. The hot air is exhausted by the fan and drift eliminators prevent droplets of water from being blown out of the tower [6].

The chiller operates on the vapor compression or vapor absorption concept. The most frequently used air conditioning cycle is the vapor compression. The low-pressure refrigerant evaporates in the evaporator to produce a cooling effect. A compressor, which often requires electrical energy, compresses the generated refrigerant vapor to condenser pressure. The high-pressure refrigerant condenses in the condenser, and the generated heat is discharged into the atmosphere/cooling tower. The condensed refrigerant is then expanded to evaporator pressure by an expansion valve to continue the cycle. There are two types of chillers, namely air-cooled and water-cooled chillers. Water-cooled chillers can be further categorized as absorption, centrifugal, helical rotary, and scroll [7]. The chiller plant consists of the compressor, condenser, expansion valve, power unit, control unit, and water box. The compressor increases the pressure of refrigerant vapor from the evaporator to the condenser. All the components are located centrally in a chiller plant room.

AHU is a main component of the central air conditioning system of commercial buildings to maintain zone temperature in a multi-zone application [1]. There are many different types of AHU, such as (1) as per location, (2) as per fan position, (3) as per mixing capability, (4) as per energy recovery, (5) as per service zone, (6) as per ducting, and (7) as per air volume. In our air conditioning and mechanical ventilation system (ACMV) context, the AHU is a draw-through, multiple zones, single duct variable air volume (VAV) AHU with mixing capability for energy recovery. The AHU is located indoors.

The variable air volume (VAV) system of the draw-through AHU modulates airflow according to the building's thermal load condition. Connected to the supply air ducts, the VAV box in each zone controls the temperature and amount of supply air necessary to maintain zone temperature in a multi-zone application [1]. A typical representation of VAV and CAV type systems is represented in Figs. 2 and 3, respectively. The main properties of the CAV system are: (1) chilled water flow to AHU coils is modulated based on return air temperature, (2) if the percentage change of cooling load of different rooms is not same, few rooms could be over-cooled or under-cooled. Similarly, the main properties of the VAV system are: (1) the opening of the VAV box damper is based on room temperature, (2) the speed of the fan is modulated based on duct pressure, (3) the chilled water valve is modulated based on the pre-set off-coil temperature of supply air, (4) suitable if the cooling load of different rooms is different.

Measurements are recorded from various points of interest within the AHU through the sensors installed. They include pressure, flow rate, temperature sensors, etc. The AHU's air handling controller (AHC) receives these readings and sends corresponding signals to the cooling coil, fans, and dampers for regulation to achieve

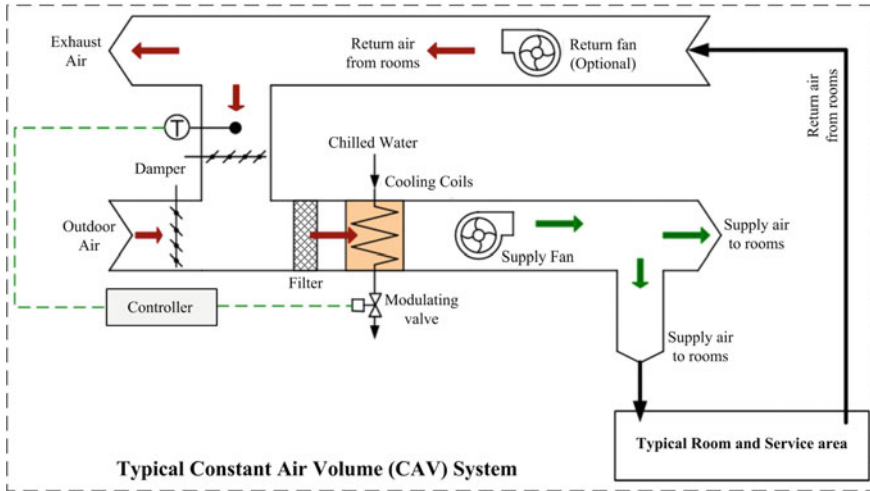


Fig. 2 Constant air volume (CAV) system’s type AHU

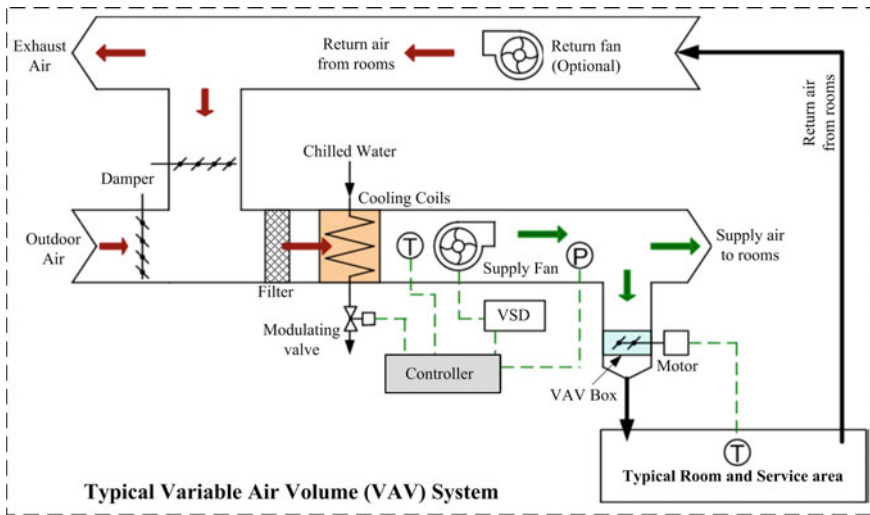


Fig. 3 Variable air volume (VAV) system’s type AHU

the designated supply air temperature and operating conditions—such as the indoor air quality (IAQ) standards. In Table 1, the functionality of each component is described.

Controlled automatically by the AHC, AHU dampers operate to conduct appropriate mixing of the air (outdoor and recirculated return air) to conserve energy by limiting heating or cooling and meeting the AIQ standards [8].

Table 1 Summary of different functionality and location of AHU components

Component		Functionality	Location
Dampers	Outdoor air damper	Damper controls the amount of air entering the AHU	Outdoor air duct
	Exhaust air damper	Controls the amount of air exhausted from the system	Exhaust air duct
	Return air damper	Controls the amount of air mixed between the outdoor air and return air	Duct between fresh air and exhaust intake
Air ducts		For the delivery of cooled/ heat air and the path back to the AHU	Building
Filter		Trap dirt and dust to prevent them from entering the building and the build-up of dust within AHU's mechanical equipment and duct	Between mixing plenum and cooling coil
Fans (draw-through)	Supply fan	Ensures enough pressure to deliver cooled air to the various zones	Located supply air duct, after cooling coil
	Return fan	Ensures enough pressure to return air from the zones to the AHU for discharging or mixing	Located at return air duct
Cooling coil		Turned on for the purpose of cooling the room to the designated temperature	In the case of the project's draw-through fan system, cooling coil is located in between the filters and supply fan
Temperature sensor	T _{OA}	Measure temperature at outdoor air duct	Outdoor air duct
	T _{RA}	Measure temperature at return air duct	Return air duct
	T _{SA}	Measure temperature at supply air duct	Supply air duct
	T _{MA}	Measure temperature after mixing plenum	After mixing plenum
Pressure sensor	Filter pressure sensor	Differential pressure sensor measures the amount of blockage in the filter due to dirt, warning engineers for a replacement	Across filter
	Fan pressure sensor (used in BMS)	Differential pressure sensor used as a gauge for fan's performance and status	Across fan

(continued)

Table 1 (continued)

Component		Functionality	Location
	Supply air duct static pressure	Measures the resistance to airflow caused by air moving through the duct. Information fed to VDS of supply fan	Supply air duct
Humidity sensor	Outdoor air humidity sensor	Measure the humidity of outdoor air	Before outdoor air
	After mixing chamber humidity sensor	Measure the humidity of mixed air	After mixing chamber
Airflow sensor	F ₁	Measure air flow of supply air duct. Information fed to VSD of return fan	Supply air duct
	F ₂	Measure air flow of return air duct. Information fed to VSD of return fan	Return air duct

$$\theta_{\text{outdoor}} = 1 - \theta_{\text{return}} = \theta_{\text{exhaust}} \quad (1)$$

where θ_{outdoor} = angle of outdoor air damper, θ_{return} = angle of return air damper, and θ_{exhaust} = angle of exhaust air damper.

In the AHU, the control of mechanical cooling and heating is sequentially programmed to synchronize with the damper control [9]. It's worth noting that when the amount of outdoor air mixed is kept to a minimum, the outdoor air damper position is at its lowest, while the return air damper position is at its highest, as shown in Eq. (1).

During the heating mode, the heating coil valve is regulated for hot water supply from a boiler to maintain the designated supply air temperature, while the cooling coil valve is closed and the dampers are modulated to keep the amount of outdoor air being mixed to a minimum while meeting minimal ventilation requirements [9].

As the outdoor air temperature increases, the sequential operation switches from heating to free cooling, cooling the building with outdoor air. The air dampers modulate in this mode to maintain the appropriate supply of air temperature [9].

As the outdoor air temperature further increases, the AHU will be unable to cool the supply air to the desired temperature using only the outside air, triggering the cooling coil valve to carry out mechanical cooling [9].

The fans located at the supply and return air ducts are equipped with a variable frequency drive (VFD) which modulates its speed, influencing the airflow within the AHU as load condition varies. The purpose of each VFD however, differs. The supply fan is modulated with the purpose of maintaining duct static pressure, while the return fan is modulated with the purpose of maintaining the airflow difference between the supply and return fans. The control signal sent to the VFD of the supply fan is based upon the duct static pressure read from the pressure sensor at the supply air duct (P1), while the control signal sent to the VFD of the return fan is based upon

the airflow reading from flow sensors (F1 and F2) located at the supply and return air duct, respectively [8].

It is good to note that all AHU components complement each other to achieve the operating conditions dictated by the AHC [1]. In the context of this study, the heating coil is excluded due to its inapplicability in tropical climates like Malaysia.

3 Brief Information of AHU Faults

Faults that occur in AHU can lead to inefficient energy consumption, occupant discomfort, and safety issues. Thus, it is necessary to utilize FDD tools to locate faults automatically. According to Bruton et al., implementing FDD technologies resulted in a total savings of €104,000 per year in 18 AHUs across four testing sites [10]. The faults that occur in AHU are also listed in the NREL project “An Open-Based Platform for Whole-Building Fault Detection and Diagnostics.” According to the NREL, the faults are ranked by the amount of energy consumed, and duct leakage was identified as a major fault because it has the second-highest energy impact [11].

The IEA Annex 25 provides a list of faults for the air mixing section, filter-coil section, fan section, and VAV boxes that are listed without regard to severity or frequency of occurrence. A preliminary survey among designers, construction engineers, and commissioning engineers was conducted in Japan in 1992 to determine the importance of various faults in AHU. Before assessing whether or not a fault is critical, there are seven factors to consider which are environmental degradation and occupant complaints, increased energy consumption, serious secondary damage, frequent occurrence, difficult detection, lengthy repair time, and costly repair [12].

A list of AHU faults from the NREL, ASHRAE RP 1312, and IEA is shown in Fig. 4. The most impactful faults resulting in increased energy consumption are included in Table 2, which was compiled from the ASHRAE and NREL reports.

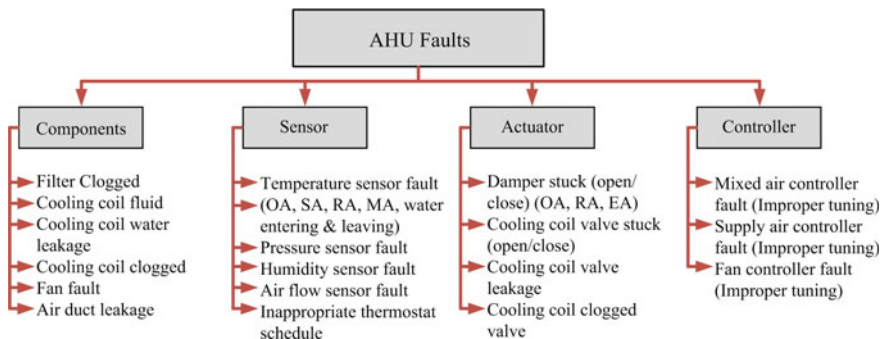


Fig. 4 List of all possible faults in AHU

Table 2 Summary of AHU faults based on NREL, IEA, and ASHRAE RP-1312 [11–13]

S.no	Fault description	Source from
1	Air duct leakage	NREL
2	Damper stuck at certain position	NREL & ASHRAE, IEA
3	Cooling coil valve stuck/leak	ASHRAE & IEA
4	Fan motor degradation	NREL & IEA
5	Fan motor failure	ASHRAE
6	Supply air (SA) temperature sensor fault	NREL & ASHRAE
7	Outdoor air (OA) temperature sensor fault	NREL & ASHRAE
8	Inappropriate set point/schedule for thermostat	NREL
9	Supply air (SA) flow rate sensor reading fault	ASHRAE
10	Supply air (SA) pressure sensor reading fault	ASHRAE

Since these ten faults impact energy consumption and indoor thermal comfort, it is critical to conduct FDD so that the ACMV system will work efficiently with minimal operating costs and a high level of comfort for the occupants.

4 Simulation of ACMV Model

OpenStudio (OS) is an open source software development kit (SDK) for building energy modeling (BEM) that intends to significantly reduce the time and effort necessary to develop and maintain BEM-based applications, as well as to extend and support the ecosystem of end-user BEM tools and services [14]. Building fault models in OS can be used to quantify the impact of faults on building performance as well as create and test FDD techniques [15].

EnergyPlus (EP) inputs and outputs are presented in OS as a dynamic, object-oriented data model with an application programming interface (API), which is a much easier construct for programs to deal with [14]. The OS Platform includes a range of GUI programs that aid in the construction of mechanical systems, simulation job, and workflow management on local workstations and high-performance computing (HPC) clusters and result visualization [16].

The US Department of Energy (DOE) small office together with the tropical weather file is used as the reference base model. The small office reference building is a single-story building with five zones plus an attic. Certain parameters such as the scheduling of occupants will be modified to represent the typical office setting in Singapore more accurately. The US DOE contributes to the development of commercial and residential building energy codes and standards by taking part in industry review and update processes and providing technical assessments to support both published model codes and proposed modifications. DOE discloses its findings in

order to guarantee that its support is transparent and that its analysis is available for public examination and use [17].

OS application facilitates the design, simulation, and review of specific building energy models by building the model. Although, not all tabs are required for modeling a building, they are generally placed in the sequence in which they are utilized along the left-hand side of the window. The tabs are listed in Table 3 [60], along with a description of their functions. The maximum outdoor air flow rate was calculated as shown in Eq. (2).

$$\text{Flow Rate}_{\text{Outdoor Air}} = \text{Ventilation Rate} \times \text{Total Floor Area} \quad (2)$$

Figure 7 depicts the simulated operation on the base model with three parameters of interest, namely the outdoor air flow fraction, outdoor air temperature (system node 27) and the various zone temperatures. It is good to note Eq. (3). An increase in the amount (Q) of return air being mixed is equivalent to a decrease in the amount of outdoor air being mixed within the mixing chamber.

$$Q_{\text{Supply Air}} = Q_{\text{Mix Air}} = Q_{\text{Outdoor Air}} + Q_{\text{Return Air}} \quad (3)$$

The designated zone temperatures are set at 23 °C from 18:00 h to 06:00 h and 25 °C otherwise. At 06:00 h, the ACMV strives to cool the zones to the designated 23 °C, mixing more return air to save energy while conducting mechanical cooling, resulting in a tremendous drop in the outdoor air flow fraction. From 06:00 h to 18:00 h, the various fluctuations are a result of the increase or decrease in infiltration levels (Fig. 8) and occupancy (Fig. 9). It is good to note that time is required for the zone to reach the designated temperature due to the thermal time constant, resulting in small modulations between the said time frame. For instance, from 13:00 h to 17:00 h, it can be seen that when the infiltration and occupancy levels remain constant, there were no modulations seen in the outdoor airflow fraction. After 18:00 h, the designated zone temperature changes from 23 to 25 °C. With the zones previously cooled to 23 °C, more outdoor air is introduced into the system for mixing, resulting in a spike in outdoor air flow fraction.

It is observed that from 20:00 h to 22:00 h, there was a linear increase in outdoor air fraction, suggesting more outdoor air being mixed. This is attributed to a drop in light scheduling seen in Fig. 10 at 20:00 h. With lesser lights present, the zones become relatively cooler compared with when more lights were on. In an attempt to maintain zone temperatures at 25 °C, more outdoor air is used for mixing resulting in an increase in outdoor air flow fraction.

Table 3 Representation of OS tabs and description

Tabs	Description	Changes made to ASHRE-based model
Site	Specify weather, lifecycle costs, and utility bills	The weather file “tropical climate” applied to the model was obtained from the EP website
Schedules	Define schedules applied to building loads	People per space floor area which was required under the people definition was modified to 0.089699 people/m ²
Constructions	Specify materials, construction assemblies, and sets	Converting cfm/ft ² to m/s, it will lead to a value of 0.003048 m/s
Loads	Define individual building loads	The heating thermostat schedule under HVAC systems has to be removed to fit in the AMCV context as the heating was not required in Malaysia. The supply air temperature was modified to 21 °C under the cooling sizing parameters
Space types	Create profiles for how spaces are occupied	“Office WholeBuilding - Sm Office Ventilation” requires the outdoor air flow per floor area
Geometry	Define the building’s exterior and interior geometries	
Building	Assign building-level defaults and exterior items	
Spaces	Assign profiles to individual spaces	
Thermal zones	Group spaces into thermal zones and assign zone equipment	The zone cooling design supply air temperature was modified to 21 °C under the cooling sizing parameters, as specified in the “Schedule” tab and it is the same as the “Deck Temperature” schedule
HVAC	Specify heating, cooling, and water systems for the building	Total floor area for this model was 11,616 ft ² . The maximum outdoor air flow rate was calculated as shown in Eq. (2). The finalized loop for the AHU can be found in Fig. 5
Variables	Specify additional simulation reporting variables	The variable tab informs the OS platform of the desired data to output during the simulation
Simulation settings	Customize simulation settings	

(continued)

Table 3 (continued)

Tabs	Description	Changes made to ASHRE-based model
Measures	Assign OS measure scripts to a workflow	The measurements tab also enables importing of individual fault type model
Run simulations	Perform a single-energy simulation	After making all of the necessary adjustments, the model may finally begin the simulation, and it will take some time for the model to generate the required output variables as specified in the variables tab
Reports	Review simulation results for a single-energy simulation	The reports tab allows users to view various types of simulated summary findings, and the annual overview pie chart can be seen in Fig. 6

5 Dataset Collection for Further Study

For the purpose of sensitivity analysis and result demonstration, three different types of datasets have been collected such as (1) simulation datasets from our OS fault simulation model, (2) real datasets from the ASHRAE RP-1043 research project by Comstock et al. [18], and (3) real datasets from the Inventory of Data Sets for AFDD Evaluation by Jessica Granderson and Guanqing Lin [19].

The dataset from ASHRAE RP-1043 contains data measured and calculated based on a 90-ton centrifugal chiller. The experiment was designed with the specifications of air conditioning and refrigeration institute (ARI) Standard 550 for centrifugal and rotary screw water-chilling packages.

The dataset from the inventory contains performance dataset generated through simulation of physical experimentation. Both simulation and physical experimentation implement a VAV AHU for generating condition-based datasets. There are other differences between the dataset as well such as the total number of data points available for the parameters. The table below summarizes the difference between the two datasets, as given in Table 4.

It is good to note that the simulation and real data is vastly different. The real data was extracted from a heating, ventilation, and air conditioning (HVAC) system, which would suggest that both heating and cooling operations are involved. The simulated data, however, only operates in the latter operation.

6 Sensitivity Analysis and Result Demonstration

Data generation is done across the four faults once the base model is made. The data is used for data correlation analysis to determine any possible connection between the parameters and the fault. All the parameters related to the system, namely air system

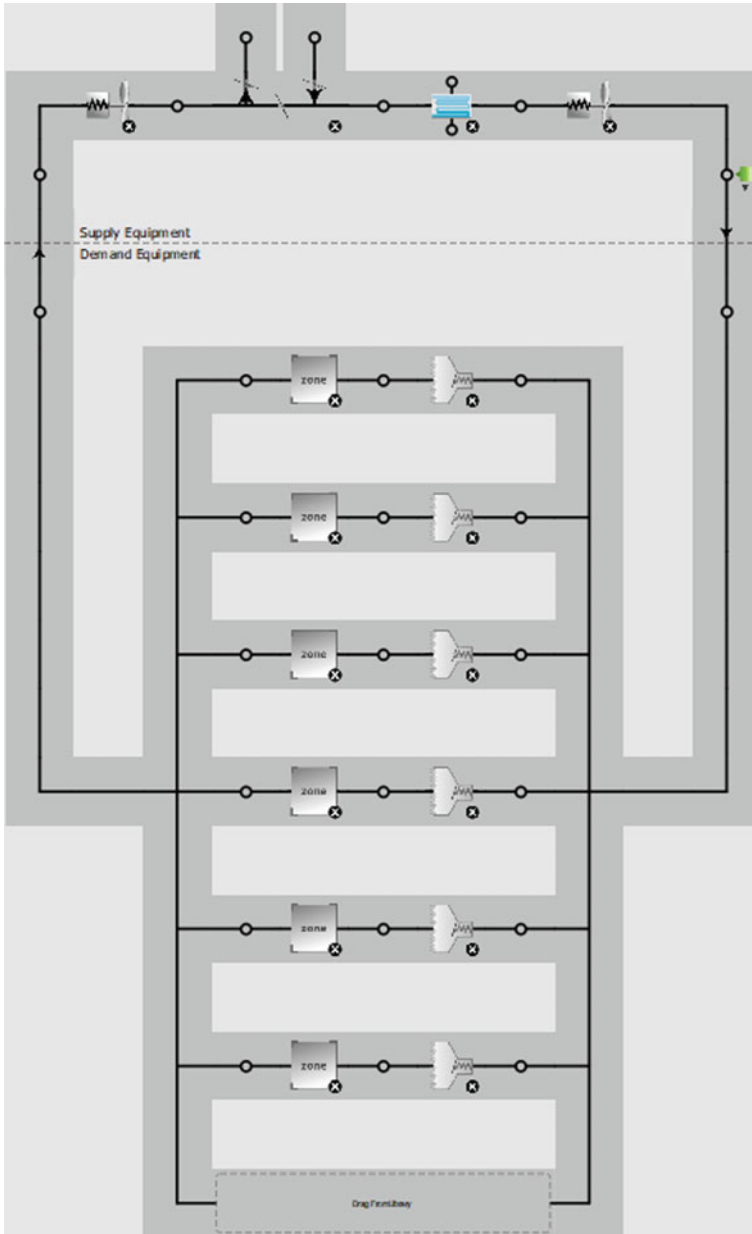


Fig. 5 Simulated AHU loop

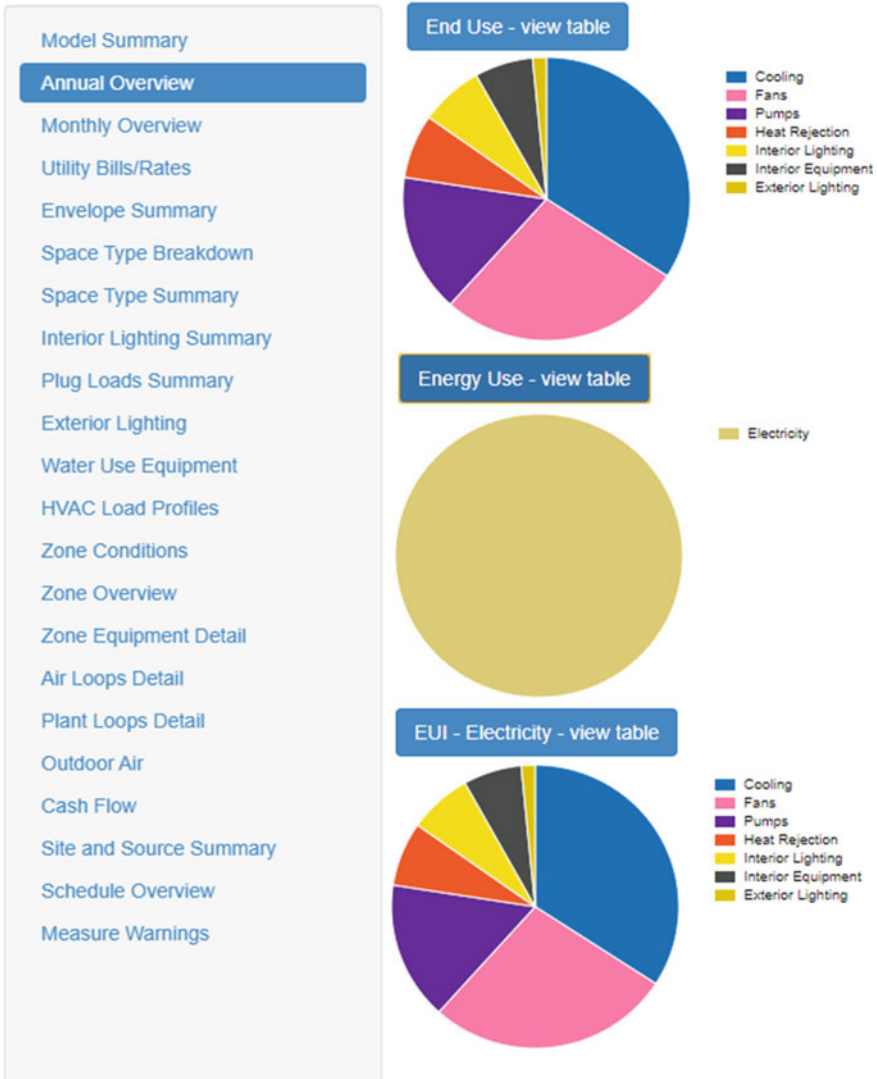


Fig. 6 Overview representation of the annual report of electrical consumption

were enabled for the analysis (in this study), followed by the model simulation. Fault propagation is captured through the enabling of parameters that are not explicitly within the system. For example, the data is generated with the consideration of the fault severity and the range of load. The range of load used is 0, 50, 100, 150, and 200% of the full load and the fault severity ranges from 0% (used as base value), 10, 20, 30, and 50% of the fault level. The collection of data is done for all the load variations and the fault severity. The collected dataset points are: (1) for cooling

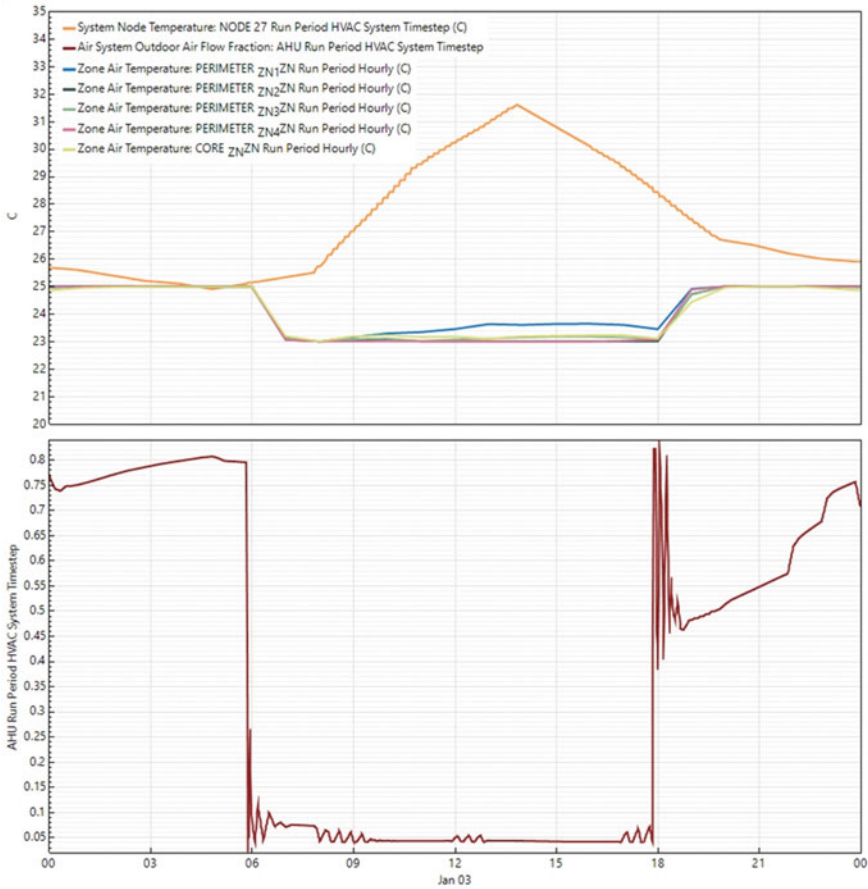


Fig. 7 Representation of outdoor air flow trends

coil (time, cooling coil total cooling energy, cooling coil source side heat transfer energy, cooling coil sensible cooling energy, cooling coil total cooling rate, cooling coil sensible cooling rate, cooling coil wetted area fraction), (2) for the fan (fan electricity rate, fan rise in air temperature, fan heat gain to air, fan air mass flow rate), and (3) air system (air system outdoor air heat recovery bypass minimum outdoor air mixed air temperature, air system outdoor air flow fraction, air system mixed air mass flow rate, air system outdoor air mechanical ventilation requested mass flow rate).

Once the data is extracted, parameters with changes according to the severity of fault and load variations are documented and arranged by its sensitivity to the varying fault levels. Sensitivity analysis is used to prioritize parameters for data dimension reduction based on the percentage difference between the average values of the parameters from the base value. The relative change formula is applied to calculate

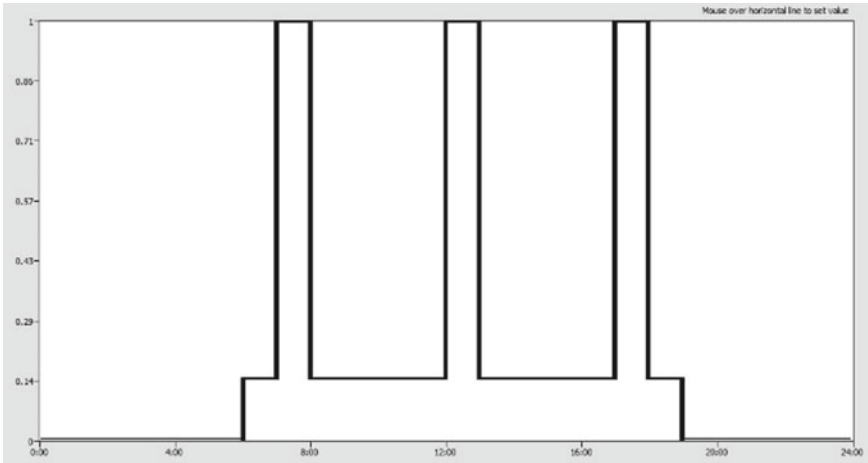


Fig. 8 Representation of door opening (infiltration) schedule

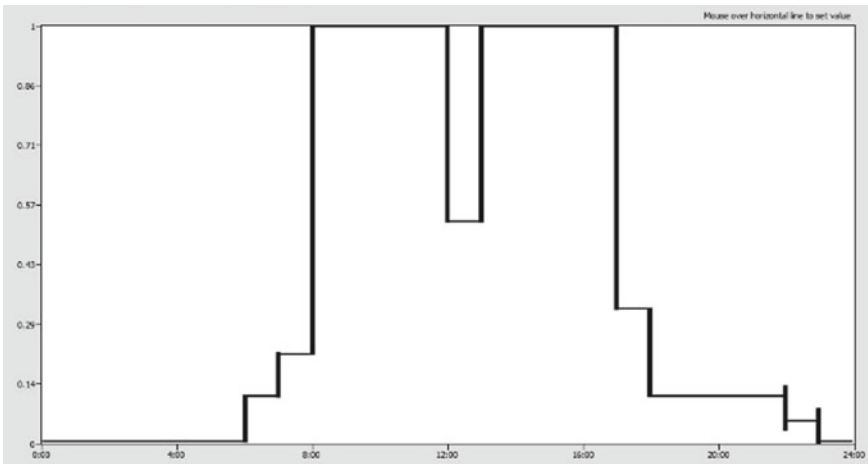


Fig. 9 Representation of occupancy schedule of building

the percentage difference between the severed parameter and the base parameter, where the final value is the average fault severed value and the initial value is the average base value for the parameter. For the case study of fan fault conditions, Table 5 gives how Eq. (4) is applied to the data, and Table 6 gives the compiled parameters with its respective sensitivity analysis.

$$\text{Relative Changes} = \left(\frac{\text{Final value} - \text{Initial value}}{\text{Initial value}} \right) \times 100 \quad (4)$$

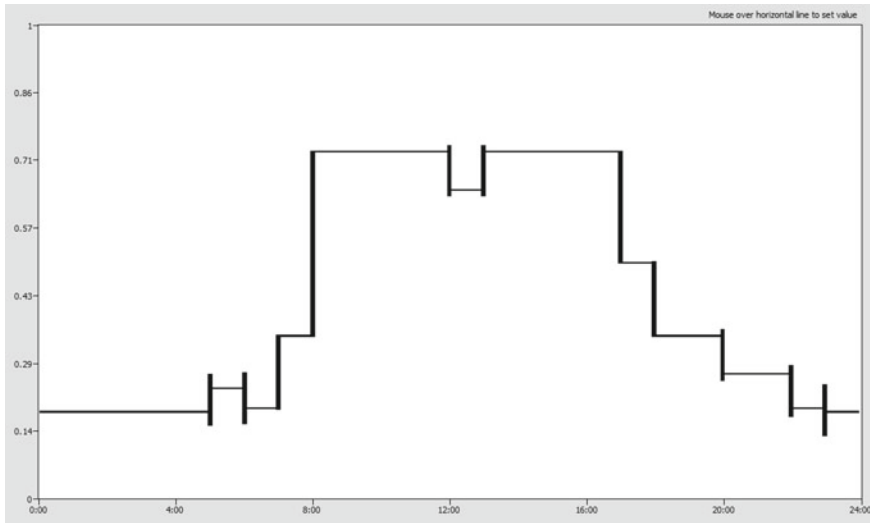


Fig. 10 Representation of building lights schedule

Table 4 Representation of differences between simulation and real datasets

Dataset	OS-based emulated dataset for AHU faults	Real dataset for each AHU faults
Number of data points	36,000	175,200
Sampling rate	1 data per min	1 data per 15 min
Time period	1 day	1 year

Similarly, for the case study of sir system fault conditions, Table 7 gives how Eq. (4) is applied to the data, and Table 8 gives the compiled parameters with its respective sensitivity analysis.

This is done to rank and identify the most sensitive parameters which will be the input for artificial intelligence (AI) and machine learning (ML)-based diagnostic models [20–30]. This is important as it simplifies and improves the accuracy of data processing. For the real data, a similar method is done for its data correlation and sensitivity. From the real data, sensitivity analysis is done by collating the average values of the parameters, and Eq. 2 is applied to calculate the percentage difference between the fault severities and the base. The ranking is then done to identify the most sensitive parameters to input for AI/ML. The selected sensitive parameters (top 10) from the simulation data and real data are represented in Table 9.

Based on Table 9, the chosen sensitive parameters are different from the simulation parameters due to the availability of the data as not all parameters are being monitored for the real system as well as the difference in system, HVAC for real data, and ACMV for simulation. However, there are overlapping parameters that are directly or indirectly related to each other. For example, in the AHU system, real data contains

Table 5 Representation of relative change formula applied for fan measurement

Fault level	M1	M2	M3	M4	M5	M6	M7	M8	M9	M10
0	2772.667	2772.667	0.941339	0.941602	2772.667	2772.667	9,981.601	9,981.601	2.767462	2.767462
0.1	3155.599	3155.599	1.048893	1.049177	3155.599	3155.599	11,360,157	11,360,157	2.774143	2.774143
0.2	3584.385	3584.385	1.177046	1.177354	3584.385	3584.385	12,903,786	12,903,786	2.749762	2.749762
0.3	4264.347	4264.347	1.352618	1.352962	4264.347	4264.347	15,351,648	15,351,648	2.766121	2.766121

M1: Fan Electricity Rate: VAR SPD FAN 3 Run Period Hourly (W), M2: Fan Electricity Rate: VAR SPD FAN 2 Run Period Hourly (W), M3: Fan Rise in Air Temperature: VAR SPD FAN 3 Run Period Hourly (delta C), M4: Fan Rise in Air Temperature: VAR SPD FAN 2 Run Period Hourly (deltaC), M5: Fan Heat Gain to Air: VAR SPD FAN 3 Run Period Hourly (W), M6: Fan Heat Gain to Air: VAR SPD FAN 2 Run Period Hourly (W), M7: Fan Electricity Energy: VAR SPD FAN 3 Run Period Hourly (J), M8: Fan Electricity Energy: VAR SPD FAN 2 Run Period Hourly (J), M9: Fan Air Mass Flow Rate: VAR SPD FAN 3 Run Period Hourly (kg/s), M10: Fan Air Mass Flow Rate: VAR SPD FAN 2 Run Period Hourly (kg/s)

Table 6 Representation of ranked parameters based on the percentage difference for fan measurement

Percentage changes	Fault level	Sensitivity analysis											
		M1	M2	M3	M4	M5	M6	M7	M8	M9	M10		
% change from base	0.1	13.81096	13.81096	11.42569	11.42477	13.81096	13.81096	13.81097	13.81097	13.81097	13.81097	0.24144	0.24144
	0.2	29.2757	29.2757	25.0396	25.0374	29.2757	29.2757	29.27572	29.27572	29.27572	29.27572	-0.63955	-0.63955
	0.3	53.79947	53.79947	43.69089	43.6873	53.79947	53.79947	53.79946	53.79946	53.79946	53.79946	-0.04844	-0.04844
% Change from 0.1	0.2	13.58809	13.58809	12.21794	12.21688	13.58809	13.58809	13.5881	13.5881	13.5881	13.5881	-0.87887	-0.87887
	0.3	35.1359	35.1359	28.9567	28.95454	35.1359	35.1359	35.13588	35.13588	35.13588	35.13588	-0.28918	-0.28918
% change from 0.2	0.3	18.97013	18.97013	14.9163	14.91546	18.97013	18.97013	18.97011	18.97011	18.97011	18.97011	0.594915	0.594915

Table 7 Representation of relative change formula applied for air system measurement

Fault level	S1	S2	S3	S4	S5	S6
0	2.54E+01	4.60E-01	2.23E-02	3.85E-01	2.77E+00	1.87E-01
0.1	2.55E+01	4.58E-01	2.23E-02	3.85E-01	2.77E+00	1.87E-01
0.2	2.56E+01	4.57E-01	2.23E-02	3.85E-01	2.75E+00	1.87E-01
0.3	2.57E+01	4.55E-01	2.23E-02	3.85E-01	2.77E+00	1.87E-01

S1: Air System Outdoor Air Heat Recovery Bypass Minimum Outdoor Air Mixed Air Temperature: AHU Run Period Hourly (C), S2: Air System Outdoor Air Flow Fraction: AHU Run Period Hourly, S3: Air System Outdoor Air Minimum Flow Fraction: AHU Run Period Hourly, S4: Air System Outdoor Air Mass Flow Rate: AHU Run Period Hourly (kg/s), S5: Air System Mixed Air Mass Flow Rate: AHU Run Period Hourly (kg/s), S6: Air System Outdoor Air Mechanical Ventilation Requested Mass Flow Rate: AHU Run Period Hourly (kg/s)

Table 8 Representation of ranked parameters based on the percentage difference for air system measurement

Percentage changes	Fault level	Sensitivity analysis					
		S1	S2	S3	S4	S5	S6
% change from base	0.1	0.3798	-0.26313	0	0	0.24144	0
	0.2	0.842727	-0.53961	0	0	-0.63955	0
	0.3	1.485053	-1.06611	0	0	-0.04844	0
% change from 0.1	0.2	0.461176	-0.27721	0	0	-0.87887	0
	0.3	1.101071	-0.8051	0	0	-0.28918	0
% change from 0.2	0.3	0.636957	-0.52936	0	0	0.594915	0

CE which is related to CCSCR in the simulation. Thus, the sensitivity analysis for simulation can be applied to a real system if the data or related data are available.

It can be noted that the real data did not contain parameter data from other sub-systems but solely on their respective sub-system, such as cooling tower data for chiller faults and pump data for AHU faults. In the simulation, Chiller and AHU faults occurring have a significant impact on the cooling tower and pump, respectively, as given in Table 9. The overall summary of effect of parameters due to fault conditions in AHU is represented in Table 10.

Table 9 Representation of sensitive parameters (selected)

Simulation data-based top sensitive parameters		Real data-based top sensitive parameters	
FD	AHU	FD	AHU
CCTCR: CCC1	CCTCR: CCC1	RASEE	RASEE
CCSCR: CCC1	CCSCR: CCC1	RASGE	RASGE
FER: VSF3	FER: VSF3	CE	CE
FER: VSF2	FER: VSF2	EF	WBFTHEDP
FRIAT: VSF3	FRIAT: VSF3	WBFTHEDP	GF
FRIAT: VSF2	FRIAT: VSF2	RSFFEE	RHCHE
FHGTA: VSF3	FHGTA: VSF3	FE	HG
FHGTA: VSF2	FHGTA: VSF2	GS	N10SNRH
FEE: VSF3	FEE: VSF3	RHCHE	N3SNRH
FEE: VSF2	FEE: VSF2	HG	RSFOSNRH
CEMFR: CEE1	CEMFR: CEE1		
PER: PVS2	PER: PVS2		
PSP:PVS2	PSP: PVS2		
PFHGR: PVS2	PFHGR: PVS2		
PMFR: PVS2	PMFR: PVS2		

CCTCR: CCC1: Cooling Coil Total Cooling Rate: CHW CLG COIL 1 Run Period HVAC System Timestep (W), *CCSCR: CCC1*: Cooling Coil Sensible Cooling Rate: CHW CLG COIL 1 Run Period HVAC System Timestep (W), *FER: VSF2*: Fan Electricity Rate: VAR SPD FAN 2 Run Period HVAC System Timestep (W), *CEMFR: CEE1*: Chiller Evaporator Mass Flow Rate: CHILLER ELECTRIC EIR 1 Run Period HVAC System Timestep (kg/s), *FEE: VSF2*: Fan Electricity Energy: VAR SPD FAN 2 Run Period HVAC System Timestep (J), *FEE: VSF3*: Fan Electricity Energy: VAR SPD FAN 3 Run Period HVAC System Timestep (J), *FER: VSF3*: Fan Electricity Rate: VAR SPD FAN 3 Run Period HVAC System Timestep (W), *FHGTA: VSF2*: Fan Heat Gain to Air: VAR SPD FAN 2 Run Period HVAC System Timestep (W), *FHGTA: VSF3*: Fan Heat Gain to Air: VAR SPD FAN 3 Run Period HVAC System Timestep (W), *FRIAT: VSF2*: Fan Rise in Air Temperature: VAR SPD FAN 2 Run Period HVAC System Timestep (delta C), *FRIAT: VSF3*: Fan Rise in Air Temperature: VAR SPD FAN 3 Run Period HVAC System Timestep (delta C), *PER: PVS2*: Pump Electricity Rate: PUMP VARIABLE SPEED 2 Run Period HVAC System Timestep (W), *PFHGR: PVS2*: Pump Fluid Heat Gain Rate: PUMP VARIABLE SPEED 2 Run Period HVAC System Timestep (W), *PMFR: PVS2*: Pump Mass Flow Rate: PUMP VARIABLE SPEED 2 Run Period HVAC System Timestep (kg/s), *PSP: PVS2*: Pump Shaft Power: PUMP VARIABLE SPEED 2 Run Period HVAC System Timestep (W)

Table 10 Representation of effect of parameters due to fault condition in AHU

Variable\Faults	Fan degradation	Return air duct leakage
<i>Overall</i>		
Electricity net: facility: site-run period hourly (J)	↑	↑
<i>In the case of fan fault analysis</i>		
Fan electricity rate: VAR SPD FAN 3 run period hourly (W)	↑	✓
Fan electricity rate: VAR SPD FAN 2 run period hourly (W)	↑	✓
Fan rise in air temperature: VAR SPD FAN 3 run period hourly (delta C)	↑	✓
Fan rise in air temperature: VAR SPD FAN 2 run period hourly (delta C)	↑	✓
Fan heat gain to air: VAR SPD FAN 3 run period hourly (W)	↑	✓
Fan heat gain to air: VAR SPD FAN 2 run period hourly (W)	↑	✓
Fan electricity energy: VAR SPD FAN 3 run period hourly (J)	↑	✓
Fan electricity energy: VAR SPD FAN 2 run period hourly (J)	↑	✓
Fan air mass flow rate: VAR SPD FAN 3 run period hourly (kg/s)	✓	✓
Fan air mass flow rate: VAR SPD FAN 2 run period hourly (kg/s)	✓	✓
<i>In the case of cooling coil fault analysis</i>		
Cooling coil total cooling energy: CHW CLG COIL 1 run period hourly (J)	↑	↑
Cooling coil source side heat transfer energy: CHW CLG COIL 1 run period hourly (J)	↑	↑
Cooling coil sensible cooling energy: CHW CLG COIL 1 run period hourly (J)	↑	↑
Cooling coil total cooling rate: CHW CLG COIL 1 run period hourly (W)	↑	↑
Cooling coil sensible cooling rate: CHW CLG COIL 1 run period hourly (W)	↑	↑
Cooling coil wetted area fraction: CHW CLG COIL 1 run period hourly	-	-
<i>In the case of air system fault analysis</i>		
Air system outdoor air heat recovery bypass minimum outdoor air mixed air temperature: AHU run period hourly (C)	↑	✓
Air system outdoor air flow fraction: AHU run period hourly	↓	↑
Air system outdoor air minimum flow fraction: AHU run period hourly	-	-
Air system outdoor air mass flow rate: AHU run period hourly (kg/s)	-	↑
Air system mixed air mass flow rate: AHU run period hourly (kg/s)	✓	✓

(continued)

Table 10 (continued)

Variable\Faults	Fan degradation	Return air duct leakage
Air system outdoor air mechanical ventilation requested mass flow rate: AHU run period hourly (kg/s)	–	–
<i>In the case of system node</i>		
Temperature: node 29		↑
Air mass flow rate: node 28		↑

Legend: ↑: Consistent Increment At Increasing Fault Severity, ↓: Consistent Decrement At Increasing Fault Severity, ✓: Both Increment & Decrement Seen During Increasing Fault Severity, –: No Correlation Seen During Increasing Fault Severity

7 Conclusion

In this chapter, data reliability analysis for early fault diagnosis of AHU is performed by using two categories of datasets (category-1 dataset: emulated data, and category-2 dataset: real-data measurement). EnergyPlus⁺-based OpenStudio software platform is used to simulate the building envelope to generate the emulated dataset under different operating scenarios. In the simulation, building operation is fixed as per the working hours of the building's user, and a dataset is generated for different fault scenarios starting from healthy condition to the most severe fault condition. The fault severity is considered from 0 to 30% w.r.t. healthy situation, and different electrical and non-electrical signals were recorded for further analysis. Based on sensitivity analysis of different signals w.r.t. the fault severity levels, the most sensitive signals have been selected, which may be used for the development of the classifier/identifier of the faults at an early stage. For the real-recorded dataset, the chosen sensitive parameters are different from the simulation parameters due to the availability of the data as not all parameters are being monitored for the real system, as well as the difference in system, HVAC for real data, and ACMV for simulation. However, there are overlapping parameters that are directly or indirectly related to each other. In the AHU system, real data contains CE which is related to CCSCR in the simulation. Thus, the sensitivity analysis for simulation can be applied to a real system if the data or related data are available.

Acknowledgements This study was supported by the Universiti Teknologi, Malaysia—"Development of Adaptive and Predictive ACMV/HVAC Health Monitoring System Using IoT, Advanced FDD, and Weather Forecast Algorithms" (Q.J130000.3823.31J06).

References

1. McDowall R (2009) Chapter 1—introduction to HVAC. In: *Fundamentals of HVAC systems: a course reader*. Elsevier, pp 1–10
2. Malik H, Panda SK, Pootla K, Spanos CJ (2022) Data-driven hybrid approach for early fault detection of AHU using electrical signals. In: *2022 international power electronics conference (IPEC-Himeji 2022- ECCE Asia)*, Himeji, Japan, pp 1365–1371. <https://doi.org/10.23919/IPEC-Himeji2022-ECCE53331.2022.9807260>
3. Chandra R et al. (2020) A survey of failure mechanisms and statistics for critical electrical equipment in buildings. In: *IECON 2020 the 46th annual conference of the IEEE industrial electronics society*, Singapore, pp 1955–1961. <https://doi.org/10.1109/IECON43393.2020.9254225>
4. Xinjie J, Malik H, Panda SK (2022) An optimized intelligent technique for bearing fault diagnosis using motor current signal analysis. In: *2022 international power electronics conference (IPEC-Himeji 2022-ECCE Asia)*, Himeji, Japan, pp 730–735. <https://doi.org/10.23919/IPEC-Himeji2022-ECCE53331.2022.9807128>
5. Malik H et al, Method and system for determining a condition of an airflow device. Patent, World Intellectual Property Organization, WO2022186770A1
6. U.S Department of Energy (2011) Cooling towers: understanding key components of cooling towers and how to improve water efficiency. Energy.gov. <https://www.coursehero.com/file/35758596/waterfs-coolingtowerspdf/>. Accessed 31 Mar 2022
7. Islam MR, Air-conditioning and mechanical ventilation (ACMV) systems. Institution of Engineers. [https://www.ies.org.sg/Tenant/C0000005/PDF%20File/Registry/SCMV/ACMV\(1\).pdf](https://www.ies.org.sg/Tenant/C0000005/PDF%20File/Registry/SCMV/ACMV(1).pdf). Accessed 24 Oct 2022
8. Seem J, House J, Kelly G, Klaassen C (2000) A damper control system for preventing reverse airflow through the exhaust air damper of variable-air-volume air-handling units. *HVAC&R Res* 6(2):135–148
9. Yu Y, Woradechjumroen D, Yu D (2014) A review of fault detection and diagnosis methodologies on air-handling units. *Energy Build* 82:550–562
10. Bruton K, Raftery P, O'Donovan P, Aughney N, Keane MM, O'Sullivan D (2014) Development and alpha testing of a cloud based automated fault detection and diagnosis tool for air handling units. *Automation in Construction*. <https://doi.org/10.1016/j.autcon.2013.12.006>. Accessed 24 Oct 2022
11. Kim J, Cai J, Braun JE (2018) Common faults and their prioritization in small commercial buildings. National Renewable Energy Laboratory. <https://www.nrel.gov/docs/fy18osti/70136.pdf>. Accessed 28 Mar 2022
12. Yoshida H (1996) Building optimization and fault diagnosis source book. In: *VAV air handling unit*, p 74. http://www.iea-ebc.org/Data/publications/EBC_Annex_25_source_book.pdf. Accessed 24 Oct 2022
13. Li T, Deng M, Zhao Y, Zhang X, Zhang C (2020) An air handling unit fault isolation method by producing additional diagnostic information proactively. <https://doi.org/10.1016/j.seta.2020.100953>. Accessed 24 Oct 2021
14. “OpenStudio,” Energy.gov, 28 Aug 2014. <https://www.energy.gov/eere/buildings/downloads/openstudio-0>. Accessed 24 Oct 2022
15. Cheung H, Braun JE (2016) Empirical modeling of the impacts of faults on water-cooled chiller power consumption for use in building simulation programs. *Appl Therm Eng* 99:756–764
16. Guglielmetti R, Macumber D, Long N (2011) OpenStudio: an open source integrated analysis platform. NREL. <https://www.nrel.gov/docs/fy12osti/51836.pdf>. Accessed 24 Oct 2022
17. Prototype building models. Building Energy Codes Program, 30 Oct 2021. <https://www.energycodes.gov/prototype-building-models>. Accessed 30 Oct 2022
18. Comstock MC et al, Experimental data from fault detection and diagnostic studies on a centrifugal chiller. In: *ASHRAE deliverable for research project 1043-RP fault detection and diagnostic (FDD) requirements and evaluation tools for chillers*, HL 99-18 Report #4036-1

19. Granderson J, Lin G (2019) Inventory of data sets for AFDD evaluation. Building Technology and Urban Systems Division Lawrence Berkeley National Laboratory
20. Azeem A et al (2022) Real-time harmonics analysis of digital substation equipment based on IEC-61850 using hybrid intelligent approach. *J Intell Fuzzy Syst* 42(2):741–754. <https://doi.org/10.3233/JIFS-189745>
21. Azeem A et al (2021) Design of hardware setup based on IEC 61850 communication protocol for detection & blocking of harmonics in power transformer. *Energies* 14(24):8284, 1–27. <https://doi.org/10.3390/en14248284>
22. Malik H, Mishra S (2017) Selection of most relevant input parameters using principle component analysis for extreme learning machine based power transformer fault diagnosis model. *Int J Electr Power Compon Syst* 45(12):1339–1352. <https://doi.org/10.1080/15325008.2017.1338794>
23. Malik H et al (2022) Data-driven hybrid approach for early fault detection of AHU using electrical signals. In: 2022 international power electronics conference (IPEC-Himeji 2022-ECCE Asia), Himeji, Japan, pp 1365–1371. <https://doi.org/10.23919/IPEC-Himeji2022-ECC53331.2022.9807260>
24. Malik H, Ahmad W, Kothari DP (2022) Intelligent data analytics for power and energy systems: advances in models and applications, 1st ed. Springer Nature, Berlin/Heidelberg, Germany. ISBN 978-981-16-6080-1
25. Malik H et al (2022) Power quality disturbance analysis using data-driven EMD-SVM hybrid approach. *J Intell Fuzzy Syst* 42(2):669–678. <https://doi.org/10.3233/JIFS-189739>
26. Fatema N et al (2022) Data driven intelligent model for quality management in healthcare. *J Intell Fuzzy Syst* 42(2):1155–1169. <https://doi.org/10.3233/JIFS-189779>
27. Fatema N, Malik H (2020) Data-driven occupancy detection hybrid model using particle swarm optimization based artificial neural network. In: Springer Nature book: Metaheuristic and evolutionary computation: algorithms and applications, under book series “Studies in computational intelligence”, pp 283–297. https://doi.org/10.1007/978-981-15-7571-6_13
28. Fatema N et al (2019) Big-data analytics based energy analysis and monitoring for multi-story hospital buildings: case study. In: Springer Nature book: Soft computing in condition monitoring and diagnostics of electrical and mechanical systems, pp. 325–343. https://doi.org/10.1007/978-981-15-1532-3_14
29. Fatema N et al (2019) Data driven intelligent model for sales prices prediction and monitoring of a building. In: Springer Nature book: Soft computing in condition monitoring and diagnostics of electrical and mechanical systems, pp. 407–421. https://doi.org/10.1007/978-981-15-1532-3_18
30. Bist V et al (2022) A data-driven intelligent hybrid method for health prognosis of lithium-ion batteries. *J Intell Fuzzy Syst* 42(2):897–907. <https://doi.org/10.3233/JIFS-189758>